Paper

Int'l J. of Aeronautical & Space Sci. 18(3), 555–564 (2017)
DOI: http://dx.doi.org/10.5139/IJASS.2017.18.3.555

IJASS
International Journal of Aeronautical and Space Sciences

Vibration-Robust Attitude and Heading Reference System Using Windowed Measurement Error Covariance

Jong-Myeong Kim*

Chosun University, Gwangju 61452, Republic of Korea

Sung-Hoon Mok**

Korea Advanced Institute of Science and Technology, Daejeon 34141, Republic of Korea

Henzeh Leeghim* and Chang-Yull Lee******

Chosun University, Gwangju 61452, Republic of Korea.

Abstract

In this paper, a new technique for attitude and heading reference system (AHRS) using low-cost MEMS sensors of the gyroscope, accelerometer, and magnetometer is addressed particularly in vibration environments. The motion of MEMS sensors interact with the scale factor and cross-coupling errors to produce random errors by the harsh environment. A new adaptive attitude estimation algorithm based on the Kalman filter is developed to overcome these undesirable side effects by analyzing windowed measurement error covariance. The key idea is that performance degradation of accelerometers, for example, due to linear vibrations can be reduced by the proposed measurement error covariance analysis. The computed error covariance is utilized to the measurement covariance of Kalman filters adaptively. Finally, the proposed approach is verified by using numerical simulations and experiments in an acceleration phase and/or vibrating environments.

Key words: AHRS (Attitude & Heading Reference System), INS (Inertial Navigation System), EKF (Extended Kalman Filter), Attitude determination

1. Introduction

Recently, the unmanned aerial vehicle (UAV) has been one of the key platforms for the various field of applications, for example, surveillance, reconnaissance, aerial photography and so on. The small sized UAVs, for example, the multi-copters are positioned on the dominant areas of research and development. Due to outstanding features of the MEMS technology, the small-sized inertial measurement unit (IMU) is able to be manufactured by MEMS accelerometers, gyroscopes, and magnetometers. The MEMS sensors have a wide range of applications due to its low cost, small size, and low power consumption. One of the drawbacks of the MEMS sensors is that they introduce relatively large measurement errors induced by the scale factor error, drift error and so on. Therefore, MEMS sensors are mixed with the external devices such as global positional system (GPS) to improve the accuracy of navigation and attitude information [1-3].

Primary knowledges required to control UAVs are the precise orientation and attitude information provided by IMUs. As mentioned above, a number of small UAVs make use of MEMS sensors since most of small-sized IMUs are comprised of low-cost MEMS sensors. It is very natural that key technologies for MEMS based IMUs are abilities to generate high quality attitude information by filtering methods as accurately as possible. Note that the attitude in a local position is in general estimated by using the direction of a gravity vector measured by accelerometers. It is quite difficult to estimate the direction of gravity vector when IMUs are under acceleration phase, since the gravity and the acceleration cannot be measured

* Graduate Student, Dept. of Aerospace Engineering
** Post Doc. Researcher, Dept. of Aerospace Engineering
*** Assistant Professor, Dept. of Aerospace Engineering
**** Assistant Professor, Corresponding Author : cylee@chosun.ac.kr

Received: May 11, 2016 Revised: April 10, 2017 Accepted: July 18, 2017

http://ijass.org pISSN: 2093-274x eISSN: 2093-2480

separately due to the inherent property of the acceleration. It makes active research possible to improve performances of MEMS IMUs as well.

One of the well-known approaches is to utilize the extended Kalman filtering (EKF) technique. The angular rate generated by the output of gyroscopes is used for the propagation, and the output of accelerometers is used for the measurement update of the EKF algorithm. If the norm of measured acceleration is different from the norm of the local gravity vector with a certain level, then the EKF assumes that the IMU is under the acceleration phase. In that case, the gravity vector could not be estimated accurately so that the EKF performs only the propagation process using the angular rates[4-9]. Much powerful technique so called adaptive Kalman Filtering (AKF) is introduced [10-11]. This algorithm handles measurement error covariance as an adaptive variable. In other words, AKF updates the measurement covariance continuously by inspecting the norm of the acceleration. That is, it analyzes the difference of norms between the gravity vector and accelerometer measurement. Note that in this approach, determination of the level of the norm difference is also important since it is deeply related to attitude performances.

A meaningful success has been accomplished in the development of attitude and heading reference systems (AHRS) using MEMS sensors. Nevertheless, most of the algorithms would fall into performance degradation in vibration environments. In a vibration environment, some vibration induced errors will average to zero. The high-frequency term of the vibration could be in general treated as the white noise since it can be averaged out. Furthermore, the low-frequency term of the vibration behaves like a drift, i.e, bias or random walk. The well-known vibration rectification error(VRE) which is induced by the asymmetric and/or nonlinearity of sensors can be regarded as the vibration induced bias[16-17]. It is quite difficult to fully respond the vibration ranging from low-frequency to high-frequency in the generic Kalman filter formulation. Therefore, it is assumed in this work that the level of the asymmetric and/or nonlinearity of sensors are low so that the VRE is negligible. In this paper, a new approach for AHRS using low-cost sensors in vibration environments is proposed. Obviously, it is very important to identify the vibration environment. The key idea is that by inspecting the set of windowed measurements, it is possibly able to estimate that the system is now under vibration environments. That is, it is much desirable to make use of a large data set to identify the vibrational environment compared with a small data set. The windowed measurement error covariance (WMEC) of a norm between windowed measurements of accelerometers and gravity vector by statistical approaches is directly employed to the measurement covariance of the extended Kalman filter adaptively.

This paper is organized as follows. A brief review on the EKF for AHRS is placed on the first section. The attitude kinematics, error dynamics for attitude estimation and measurement update for EKF are illustrated in this section. Next, the proposed algorithm of WMEC in this paper is explained and employed to the Kalman filter technique. Then, the suggested technique is verified by numerical simulations and experiments as well. Finally the last section illustrates conclusions of this paper.

2. Attitude and Heading Reference System

In this section, the attitude and heading reference system based on the EKF is briefly introduced for the augmentation to the proposed WMEC algorithm.

2.1 Attitude Kinematics

In this part the basic properties of attitude kinematics are briefly summarized. There are a variety of ways to express the attitude, for example, direction cosine matrix (DCM), quaternion, Euler angles, Euler axis and rotation angles, Rodrigues, and so on. Since DCM has relatively many entities to identify in the matrix, and the Euler angle representation has a singularity problem, Therefore, the quaternion for attitude representations can be the primary choice in this paper since the quaternion has useful advantages of a small nonlinearity and no singularity.

Firstly, let us briefly review the attitude representation. The quaternion is defined as

$$\mathbf{q} = \begin{bmatrix} \mathbf{p}^T & q_4 \end{bmatrix}^T, \tag{1}$$

where the quaternion is comprised with a vector part and a scalar part. The quaternion inverse is also given by

$$\hat{\mathbf{q}}^{-1} = \begin{bmatrix} -\hat{\mathbf{p}}^T & \hat{q}_4 \end{bmatrix}^T. \tag{2}$$

Since the four-dimensional vector is used to describe a three-dimensional space, the quaternion needs to obey the norm constraint given by

$$\mathbf{q}^T\mathbf{q} = q_1^2 + q_2^2 + q_3^2 + q_4^2 = 1. \tag{3}$$

Even though the quaternion must keep the norm constraint, it can be resolved numerically by the normalization process in actual applications. The relationship between DCM and quaternion is given by

$$C(\mathbf{q}) = \Xi^T(\mathbf{q})\Psi(\mathbf{q}), \tag{4}$$

where

$$\Xi(\mathbf{q}) = \begin{bmatrix} q_4 I_{3\times3} + [\mathbf{p}\times] \\ -\mathbf{p}^T \end{bmatrix}, \quad \Psi(\mathbf{q}) = \begin{bmatrix} q_4 I_{3\times3} - [\mathbf{p}\times] \\ -\mathbf{p}^T \end{bmatrix}, \tag{5}$$

and $I_{3\times3}$ is an identity matrix, and the bracket $[\mathbf{p}\times]$ represents the skew-symmetric matrix defined as

$$[\mathbf{p}\times] = \begin{bmatrix} 0 & -q_3 & q_2 \\ q_3 & 0 & -q_1 \\ -q_2 & q_1 & 0 \end{bmatrix}. \tag{6}$$

Note that the advantage of quaternions is that successive rotations can be accomplished just by using simple quaternion multiplications

The quaternion kinematic model is given by [12]-[15]

$$\dot{\mathbf{q}} = \frac{1}{2}\Omega(\boldsymbol{\omega})\mathbf{q} = \frac{1}{2}\Xi(\mathbf{q})\boldsymbol{\omega}, \tag{7}$$

where $\boldsymbol{\omega} = \begin{bmatrix} \omega_x & \omega_y & \omega_z \end{bmatrix}^T$ is the angular rate vector, and the transformation matrices Ω is defined as

$$\Omega(\boldsymbol{\omega}) = \begin{bmatrix} -[\boldsymbol{\omega}\times] & \boldsymbol{\omega} \\ -\boldsymbol{\omega}^T & 0 \end{bmatrix}. \tag{8}$$

Since the overall representation of the quaternion kinematics are bilinear, it is much computationally efficient rather than other attitude kinematics.

2.2 State Propagation

A three-axis gyroscope, accelerometer, and magnetometer are used to realize an ARHS system in this paper. The quaternion for attitude and gyro bias are considered to be estimated for AHRS. A nonlinear model needs to be linearized to apply for the extended Kalman filtering technique. Since quaternions are quasi-linear, it is required to be represented an error state model. Let us first formulate attitude error representation. The quaternion error, $\delta\mathbf{q}$, is given by

$$\delta\mathbf{q} = \mathbf{q} \otimes \hat{\mathbf{q}}^{-1}, \tag{9}$$

where $\otimes$ denotes quaternion multiplication, $\mathbf{q}$ represents a true quaternion ,and $\hat{\mathbf{q}}$ is an estimated quaternion. Next, let us differentiate the error quaternion with respect to time and insert the quaternion kinematics in Eq.(7). Then the vector part of the error quaternion leads to [12]

$$\delta\dot{\mathbf{p}} = -[\hat{\boldsymbol{\omega}}\times]\delta\mathbf{p} + \frac{1}{2}\delta\boldsymbol{\omega}, \tag{10}$$

where $\hat{\omega}$ denotes the estimation angular velocity vector. This linearized attitude error model in Eq.(10) will be used for the propagation of the EKF technique. Note that the error of quaternion fourth component remains constant.

The gyroscope measurement model is in general given by

$$\boldsymbol{\omega} = \tilde{\boldsymbol{\omega}} - \boldsymbol{\beta} - \mathbf{w}_g, \tag{11a}$$

$$\dot{\boldsymbol{\beta}} = \mathbf{w}_{gb}, \tag{11b}$$

where, $\boldsymbol{\omega}$ and $\hat{\boldsymbol{\omega}}$ are true angular rate vector and measured angular rate vector, respectively, and $\boldsymbol{\beta}$ denotes the gyro bias derived from the first order Markov process, and $\mathbf{w}_g$, $\mathbf{w}_{gb}$ are zero-mean white Gaussian noises of the gyro angular rate and gyro bias with spectral densities of $\sigma_g I_{3\times3}$ and $\sigma_{gb} I_{3\times3}$, respectively.

For the standard EKF formulation, the estimated angular rate ($\hat{\boldsymbol{\omega}}$) and the mean of the differential equation of gyro bias are described as

$$\hat{\boldsymbol{\omega}} = \tilde{\boldsymbol{\omega}} - \hat{\boldsymbol{\beta}}, \tag{12}$$

and

$$\dot{\hat{\boldsymbol{\beta}}} = 0. \tag{13}$$

By using Eqs.(10) and (11), the angular rate error vector is given by

$$\delta\boldsymbol{\omega} = -\Delta\boldsymbol{\beta} - \mathbf{w}_g. \tag{14}$$

where the angular rate error and the bias error are defined as $\delta\boldsymbol{\omega}=\hat{\boldsymbol{\omega}}-\tilde{\boldsymbol{\omega}}$ and $\Delta\boldsymbol{\beta} = \boldsymbol{\beta} - \hat{\boldsymbol{\beta}}$, respectively. Then, substituting Eq.(14) into Eq. (10) leads to

$$\delta\dot{\mathbf{p}} = -[\hat{\boldsymbol{\omega}}\times]\delta\mathbf{p} - \frac{1}{2}\left(\Delta\boldsymbol{\beta} + \mathbf{w}_g\right). \tag{15}$$

Let us assume that the attitude error is small. By the small angle approximation, the vector part of the quaternion error can be simply approximated by Euler angles :

$$\delta\mathbf{p} \approx \frac{\delta\boldsymbol{\alpha}}{2} = \frac{1}{2}\begin{bmatrix} \delta\phi \\ \delta\theta \\ \delta\psi \end{bmatrix}, \tag{16}$$

where $\delta\boldsymbol{\alpha}$ is the Euler angle vector comprised of roll, pitch, yaw error angles for any rotation sequence. By using this simplified equation, Eq.(15) can be rewritten as

$$\delta\dot{\boldsymbol{\alpha}} = -[\hat{\boldsymbol{\omega}}\times]\delta\boldsymbol{\alpha} - \left(\Delta\boldsymbol{\beta} + \mathbf{w}_g\right). \tag{17}$$

This approach gives a direct physical meaning to the state error covariance, which can be used to directly determine 3σ deviation of actual attitude errors.

The standard EKF error model for the state propagation is given by

$$\Delta\dot{\tilde{\mathbf{x}}} = F(t)\Delta\tilde{\mathbf{x}} + G(t)\mathbf{w}(t). \tag{18}$$

where the transformation matrix and state variables are defined as [12]

$$\Delta\tilde{\mathbf{x}}(t) = \begin{bmatrix} \delta\boldsymbol{\alpha}^T(t) & \Delta\boldsymbol{\beta}^T(t) \end{bmatrix}^T, \tag{19a}$$

$$\mathbf{w}(t) = \begin{bmatrix} \mathbf{w}_g^T & \mathbf{w}_{gb}^T \end{bmatrix}^T, \tag{19b}$$

$$F(t) = \begin{bmatrix} -[\boldsymbol{\omega}\times] & -I_{3\times3} \\ 0_{3\times3} & 0_{3\times3} \end{bmatrix}, \tag{19c}$$

$$G(t)=\begin{bmatrix} I_{3\times3} & 0_{3\times3} \\ 0_{3\times3} & I_{3\times3} \end{bmatrix}. \tag{19d}$$

In this work the attitude error of Euler angles and gyro bias are selected as state variables to be estimated for the attitude and heading reference system. By assuming that the angular rate is constant in a given time interval Δt, the exact solution of the state transition matrix of Eq.(19c) is obtained by using the inverse Laplace transformation :

$$\begin{aligned}\Phi &= \mathcal{L}^{-1}\left[\left(sI-F\right)^{-1}\right] \\ &= \begin{bmatrix} \Phi_1 & \Phi_2 \\ 0_{3\times3} & I_{3\times3} \end{bmatrix},\end{aligned} \tag{20}$$

where the angular vector and the magnitude of the vector are defined as $\theta=\omega\Delta t$ and $\theta=\|\theta\|$, respectively, and the sub-matrices of the state transition matrix are given by

$$\Phi_1 = I_{3\times3} - [\boldsymbol{\theta}\times]\frac{\sin\theta}{\theta} + [\boldsymbol{\theta}\times]^2\frac{1-\cos\theta}{\theta^2}, \tag{21}$$

and

$$\Phi_2 = -\Delta t\left(I_{3\times3} - [\boldsymbol{\theta}\times]\frac{1-\cos\theta}{\theta^2} + [\boldsymbol{\theta}\times]^2\frac{\theta-\sin\theta}{\theta^3}\right). \tag{22}$$

The detailed derivation of the state transition matrix in Eq.(20)-(22) is placed in Appendix of this paper.

2.3 Measurement Update

Most of AHRS based on EKF utilize acceleration vectors and magnetic field vectors for the measurement update. The measurement vector of accelerometers and magnetometers are simply described as

$$\mathbf{y}=\begin{bmatrix} \mathbf{m}_b \\ \mathbf{a}_b \end{bmatrix}+\begin{bmatrix} \boldsymbol{\eta}_m \\ \boldsymbol{\eta}_a \end{bmatrix}, \tag{23}$$

where $\mathbf{m}_b$ denotes the output vector of 3 axis magnetometers and $\mathbf{a}_b$ represents the measurement vector for 3 axis accelerometers, and $\boldsymbol{\eta}_a$ and $\boldsymbol{\eta}_m$ are zero-mean white Gaussian noise vectors of the accelerometer and magnetometer with their covariance of $\sigma_g I_{3\times3}$ and $\sigma_m I_{3\times3}$, respectively. The measurement covariance (R_0) matrix for the measurement is defined as

$$R_0=\begin{bmatrix} \sigma_m I_{3\times3} & 0_{3\times3} \\ 0_{3\times3} & \sigma_a I_{3\times3} \end{bmatrix}. \tag{24}$$

Note that it is easy to calculate the measurement sensitivity matrices directly from Eq.(23).

The key feature of AHRS is to estimate the attitude and headings under the acceleration phase. The well-known approaches is to utilize the norm error level between the local gravity vector and the output of accelerometer. The AKF algorithm modifies the measurement covariance adaptively. That is, AKF updates the measurement covariance continuously by inspecting the norm error. If the magnitude of the norm error is bigger than a permissible level, the technique decrease the measurement covariance and vice versa. In this approach, determination of the level of the norm difference is also important since it is deeply relevant to the attitude performance. Nevertheless, the AKF algorithm would fall into performance degradation in a vibrational environment. Since the dynamic motion of MEMS IMU will interact with the scale factor and cross-coupling errors to produce additional random errors in the harsh environment. It means that a reliable technique is essential to properly make up for the performance degradation of the sensors due to the vibration which is a different type of acceleration.

3. Windowed Measurement Error Covariance

In this section, a new approach for AHRS in a vibration environment is addressed. As discussed in the previous section, it is very important to identify the vibration environment for attitude estimation using the MEMS based inertial sensors. The key idea is that by inspecting the set of windowed measurements it is able to recognize that the body installed with IMU is now under vibration environments. It is natural that using a large set of measurements is an appropriate idea rather than using a single measurement. The proposed algorithm in this work is to modify the measurement covariance of the AKF for AHRS adaptively. The way of computing the measurement covariance is as follows. The proposed windowed measurement error covariance (WMEC) of the norm error between the moving windowed measurement set and gravity vector is calculated by the statistical approach. Then, the computed WMEC are added onto the nominal measurement covariance R_0 with weighting parameters.

The proposed WMEC technique employs a number of N previous measurements as well as the present measurement to evaluate the adaptive measurement covariance for EKF algorithm. That is, the WMEC approach demands all the measurements obtained between $t_{k\text{-}N}$ and t_k illustrated in Fig 1. Firstly, the way of computing the norm error of the measurement vector and the gravity vector at time t_j is given by

$$\alpha_j = \left|\sqrt{\mathbf{a}_b(t_j)^T\mathbf{a}_b(t_j)} - \sqrt{\mathbf{a}_n^T\mathbf{a}_n}\right|, \tag{25}$$

where $\mathbf{a}_b(t_j)$ presents the accelerometer output vector at time t_j and $\mathbf{a}_n$ denotes the acceleration vector of gravity at a local navigation frame. The first term in the right-hand side of the equation is the magnitude of measured accelerometer at

time t_j and the last term is the norm value of a local gravity vector. The norm error in Eq.(25) represents how much the magnitude of the measured accelerometer vector at a given time is different from that of the gravity vector. If the body frame is in the acceleration phase and/or vibration environment, the norm error at a certain time would be increased compared with nominal cases. Recall that it is a challenging problem to distinguish the vibrational parameter from the acceleration phase with the single norm error.

By modifying the measurement covariance in Eq.(24), the suggested WMEC technique is described as

$$R = R_0 + \begin{bmatrix} 0_{3\times3} & 0_{3\times3} \\ 0_{3\times3} & \lambda\left(\sum_{j=0}^{N}\gamma_j\alpha_{k-j}^2\right)I_{3\times3} \end{bmatrix}, \tag{26}$$

where λ and γ_j are the design parameters. Especially, by simply setting γ_j=1/(N+1), the summation term in Eq.(26) leads to the variance of the norm error. It is obvious that there are a variety of way to determine γ_j so that the features of the Kalman filtering also depends on the parameters under the acceleration phase. Also, the design parameter λ plays very important role as the balancing factor between the nominal covariance and the covariance of accelerometer norm error. Let us suppose that the balancing factor is selected as a small value. It is intended that the contribution of the WMEC technique would be small. In case of N=0 the WMEC will be the identical approach to the previous AKF algorithm since it makes use of only the present measurement.

A useful technique is addressed to figure out how to distinguish the vibration and acceleration phase. It is possible to evaluate the mean and covariance of α_i with N measurements. It could be assumed that the current status is acceleration phase if the mean value of the windowed measurement is larger than a certain mean level. Likewise, it is also regarded as vibrational phase if the covariance for the N measurements in Eq.(26) is larger than a certain covariance reference. Therefore, the parameter λ needs to be adjusted adaptively to avoid the fillter divege, especially, when the sensors are under the accelerational phase. In this case, relatively large value of λ is recommeded rather than the case of the vibrational environment.

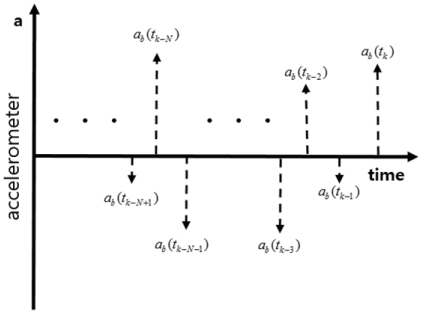

Fig. 1. Sequential Measurement of Accelerometer

Next, additional measurements can be also handled by the WMEC technique. For example, let us consider the distortion of magnetometers due to the magnetic field interference. The magnitude of the magnetic vector will be varied around the magnetic interference source. To overcome this problem, Eq.(26) can be rewritten as

$$R = R_0 + \begin{bmatrix} \kappa\left(\sum_{j=0}^{N}\mu_j\varpi_{k-j}^2\right)I_{3\times3} & 0_{3\times3} \\ 0_{3\times3} & \lambda\left(\sum_{j=0}^{N}\gamma_j\alpha_{k-j}^2\right)I_{3\times3} \end{bmatrix}, \tag{27}$$

where κ and μ_j are the design parameters for magnetometers. The norm error between the magnitude of magnetometer vector and that of a local magnetic field vector is also given by

$$\varpi_j = \left|\sqrt{\mathbf{m}_b(t_j)^T\mathbf{m}_b(t_j)} - \sqrt{\mathbf{m}_n^T\mathbf{m}_n}\right|, \tag{28}$$

where is $\mathbf{m}_b(t_j)$ presents the magnetometer output vector at time t_j and $\mathbf{m}_n$ denotes the magnetic field vector at a local navigation frame.

4. Numerical Simulations

In this section, several numerical simulations are performed to evaluate the performance of the proposed WMEC technique in the presence of acceleration and/or vibrational disturbances. The MEMS based sensors used in this simulation are chosen as 3-aixs gyroscopes, accelerometers and magnetometers. The typical specification of the MEMS sensors is listed in Table. 1. It is assumed that there is no bias terms of accelerometer and magnetometer except gyroscopes since they are unobservable with these sensor combinations. The update frequency of the sensors is selected as 10Hz for the measurement update of the Kalman filtering technique.

As discussed, the dynamic motion of MEMS IMU is going to interact with the scale factor and cross-coupling errors in vibration environments. Furthermore, some nonlinear effects are also going to introduce additional errors known as

Table 1. Typical specification of the MEMS sensors.

	Std. deviation(1σ)	Bias random walk
Gyroscope	0.06 deg/s	5 deg/h
Accelerometer	4 mg	-
Magnetometer	3 mGauss	-

VRE, and it behaves like a bias. In this work, the vibrational noise is the random Gaussian by assuming that the nonlinearity of the sensors is small in this study. To evaluate the performance of the proposed algorithm, a flight scenario is displayed in Table 2. Note that there are sinusoidally maneuvering acceleration phase for about 70 seconds and random vibration phase for about 100 seconds, respectively.

Where ω_i is the acceleration frequencies. For these simulation, ω_1 is selected as 0.2rad/s and ω_2, ω_3 are 0.1rad/s, respectively. In this study, the suggested technique is compared with the EKF algorithm for the conventional AHRS technique known as a very robust approach under the acceleration phase. Using the given scenario, a simulation is performed, and the plots of the 3-axis attitude and gyro bias errors of the EKF approach are displayed in Fig. 2 and 3. In case of the nominal condition, the errors of the attitude and gyro bias are converged within the theoretical 3σ bounds satisfactorily. The red line indicates the state error covariance. On the other hand, the errors are increased in the sinusoidal acceleration periods. Of cause it is very natural since the algorithm do not utilize the measurement update of the Kalman filtering on the acceleration phase. Therefore, one can see that the state error covariance is also increased. Much interesting results are on the interval of vibrational environments. Due to the random vibration, the EKF sometime proceeds the measurement update since the norm error is within the permissible level. Therefore, the state error covariance is smaller than the case of the acceleration phase. However, the erroneous measurement causes the state error increase. The reason is that there is a mismatch between the actual measurement and the measurement covariance of the EKF.

Next, the WMEC technique for AHRS suggested in this paper results in Fig. 4 and 5. For these simulations, γ is selected as 1, λ is 0.09, and N is chosen as 5 for the windowing. If it is regarded as an acceleration phase, λ is chosen as 10 in this case study. Note that the measurement covariance of EKF is updated adaptively by using Eq.(26) in these studies. Most promising outcome by these simulations for actual implementations is that state errors are within the theoretical covariance bounds. Of cause the error covariance is slightly increased to fit measurement qualities in the presence of acceleration phase. The emphasis on this technique is that the estimated attitude and gyro bias are always of reliable information with respect to the computed

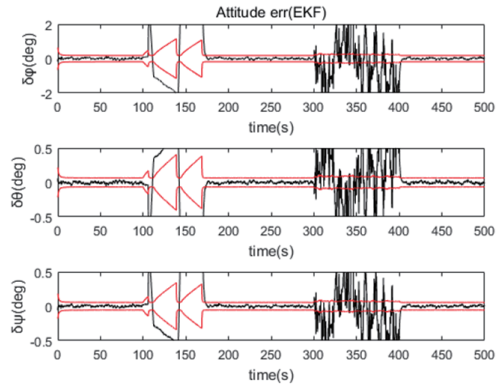

Fig. 2. Attitude error history of EKF

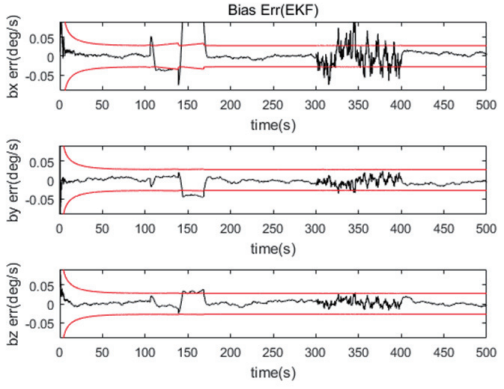

Fig. 3. Gyro bias error history of EKF

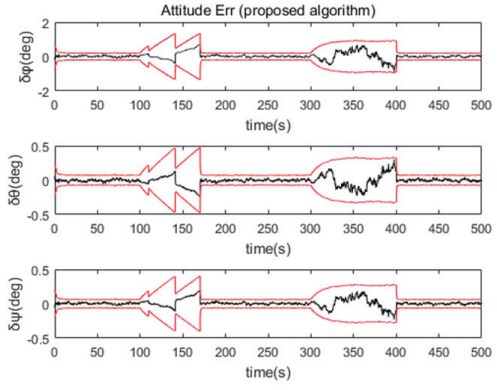

Fig. 4. Attitude error history of proposed WMEC

Table 2. Simulation Scenario

Times(sec)	External disturbance	Comments
100~170	$\left[2\sin(\omega_1 t) \quad 3\cos(\omega_2 t) \quad -2\cos(\omega_3 t)\right]^T$	Variation acceleration
300~400	$1\ m/s^2 \quad (1\sigma)$	Random vibration

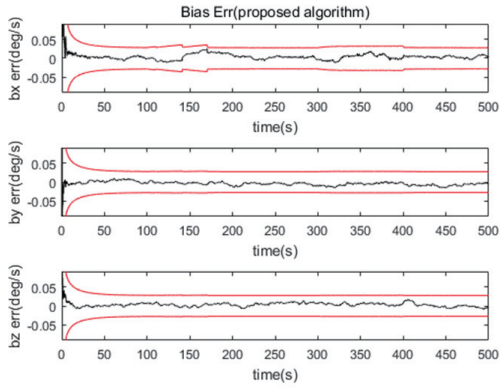

Fig. 5. Gyro bias error history of proposed WMEC

state error covariance, while the previous approaches are not. Consequently, it is obvious that the proposed algorithm can estimate the state variables reliably rather than the EKF technique, especially, in the presence of the vibration.

5. Experiments

In this section, an experiment is carried out to verify the effectiveness of the suggested technique. A test based on the conventional EKF approach is also conducted analogous to the simulation study. The sensor utilized in this experiment is a MPU9150 sensor manufactured by a three-axis accelerometer, a three-axis gyroscope and a three-axis magnetometer. The given specifications of the AHRS are listed in Table 3.

The experimental setup installed for this work is consisted of an AHRS sensor and a small motor on a 40cm board. The sensor is attached on this board. The AHRS sensor is comprised with three-axis gyroscope, three-axis accelerometers, and three-axis magnetometers. The motor is configured to operate at a constant rpm to generate vibration due to the off-centered mass. Note that to obtain the reference angle to obtain the errors, only static condition is considered for this ground experiment.

The plots of the attitude and gyro bias errors by the EKF based experiment are displayed in Fig. 6 and 7. The

Table 3. specification of MPU9150

	Std. deviation(1σ)
Gyroscope	0.06 deg/s
Accelerometer	4 mg
Magnetometer	3 mGauss

random vibration for these experiments are also added for all the time of experiments. Note that the true value of gyro bias is regarded as a constant in these experiments since the total accomplished time of the test is relatively short. It is turned out that both of attitude and bias errors are similar with the results of numerical simulation cases. That is, the errors are increased in the vibration disturbance periods much exceeding the state error covariance, while the attitude and bias errors in nominal conditions are small and bounded within the given error covariance comparatively. The red line also indicates the state error covariance.

With the same data conducted for the EKF experimental test, attitude and gyro bias are determined by using the WMEC technique with the same values of the parameters for the above simulation study once again. The plots are illustrated in Fig. 8 and 9. Needless to say, all state errors are small and the algorithm is stable considerably. Careful examination of the plots provides that error covariance of the attitude is slightly bigger than the case of the EKF. It is also attributed to the added measurement error covariance in Eq.(26). It is much theoretical since the quality of sensor measurement is assumed to be of inferior under the external acceleration and vibration environment. Finally,

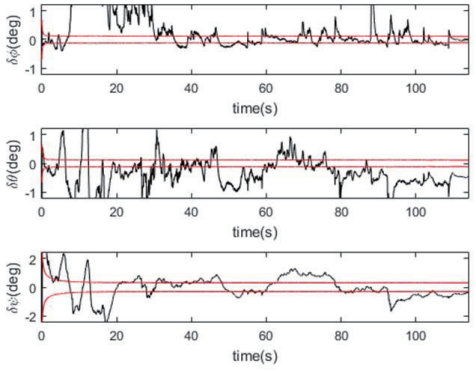

Fig. 6. Experimental attitude error of EKF

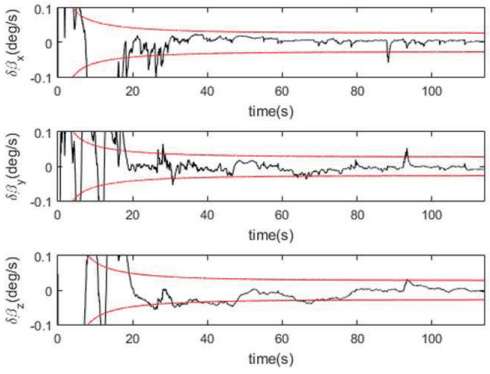

Fig. 7. Experimental gyro bias error of EKF

it is clear that the proposed technique allows small state errors, while the previous EKF technique fails to estimate the attitude and gyro bias under external disturbances, such as vibration.

Finally, the error histories of Euler angles for the EKF and the proposed WMEC technique are illustrated in Fig. 10 respectively. Note that the attitude norm error in this plot is defined as

$$\delta\alpha = \sqrt{\delta\theta^2 + \delta\phi^2 + \delta\psi^2}\,. \tag{29}$$

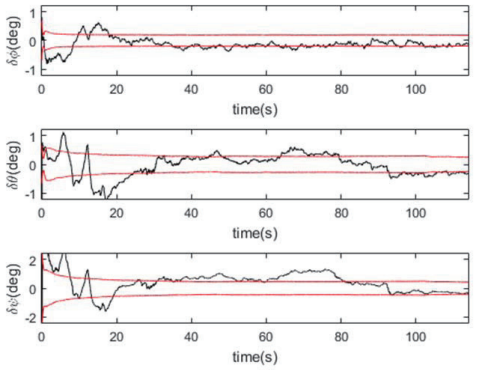

Fig. 8. Experimental attitude error of proposed WMEC

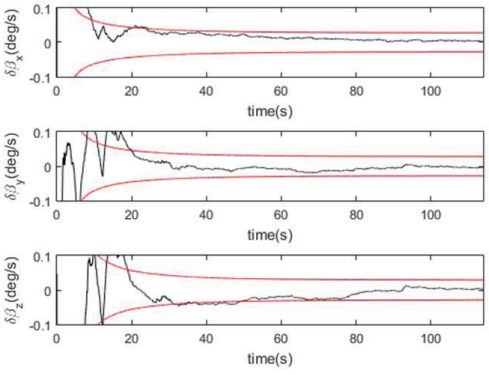

Fig. 9. Experimental gyro bias error of proposed WMEC

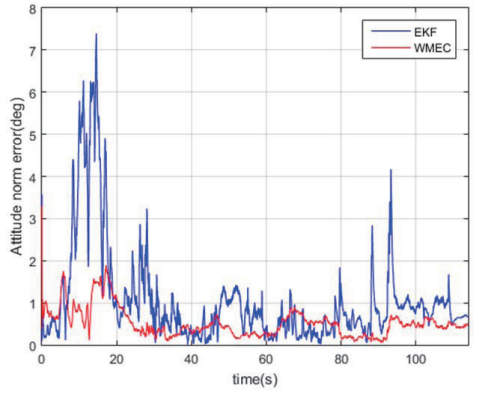

Fig. 10. Comparison of attitude norm error

The attitude error of the EKF can be sometimes smaller than that of the proposed algorithm. However, the WMEC technique in general produces a rather small amount of attitude errors stably.

6. Conclusions

A new approach for attitude and heading reference systems (AHRS) manufactured by low-cost MEMS sensors was proposed to overcome the performance degradation of attitude estimation under vibrational environments. Note that an absolute reference system is required to identify the accelerometer bias term. In this work, the proposed algorithm to estimate the attitude and angular rate only used only inertial measurement devices such as, gyroscope, accelerometers, and magnetometers so that it was assumed that the bias of accelerometer is negligible. The proposed windowed measurement error covariance (WMEC) technique employed a number of N previous measurements as well as the present measurement to compute measurement covariance for the extended Kalman filtering for AHRS. It was proven by numerically and experimentally that the WMEC method by adaptively updating measurement covariance could counteract effects of vibrational environments. Furthermore, one of leading advantages is that the suggested approach is easily implementable to the previous EKF algorithm for AHRS.

Acknowledgements

This work was supported by the National Research Foundation Grant (NRF-2015R1D1A1A01058978), Republic of Korea. Authors fully appreciate research funds.

Appendix

In this Appendix, the state transition matrix of Eq.(22) is derived in detail

$$F(t) = \begin{bmatrix} -[\boldsymbol{\omega}(t)\times] & -I_{3\times3} \\ 0_{3\times3} & 0_{3\times3} \end{bmatrix}. \tag{A1}$$

By using the inverse Laplace transformation technique, the state transition matrix is readily obtained as

$$\begin{aligned} \Phi &= L^{-1}\left[(sI - F)^{-1}\right] \\ &= L^{-1}\left(\begin{bmatrix} sI_{3\times3} + [\boldsymbol{\omega}\times] & -I_{3\times3} \\ 0_{3\times3} & sI_{3\times3} \end{bmatrix}^{-1}\right). \end{aligned} \tag{A2}$$

The magnitude of the angular rate vector is defined as $\|\boldsymbol{\omega}\| = \sqrt{\omega_x^2 + \omega_y^2 + \omega_z^2}$ and let us assuming that the angular rate is constant in a given time interval Δt. Then the inverse of the matrix given in parentheses in Eq.(A2) can be expressed as

$$(sI - F)^{-1} = \begin{bmatrix} \Psi_1 & \Psi_2 \\ 0_{3\times3} & \frac{1}{s} I_{3\times3} \end{bmatrix}, \tag{A3}$$

where

$$\Psi_1 = \frac{1}{s\left(s^2 + \|\boldsymbol{\omega}\|\right)} \begin{bmatrix} s^2 + \omega_x^2 & \omega_x\omega_y + s\omega_z & \omega_x\omega_z - s\omega_y \\ \omega_x\omega_y - s\omega_z & s^2 + \omega_y^2 & \omega_y\omega_z + s\omega_x \\ \omega_x\omega_z + s\omega_y & \omega_y\omega_z - s\omega_x & s^2 + \omega_z^2 \end{bmatrix}, \tag{A4a}$$

$$\Psi_2 = \frac{-1}{s^2\left(s^2 + \|\boldsymbol{\omega}\|^2\right)} \begin{bmatrix} s^2 + \omega_x^2 & \omega_x\omega_y + s\omega_z & \omega_x\omega_z - s\omega_y \\ \omega_x\omega_y - s\omega_z & s^2 + \omega_y^2 & \omega_y\omega_z + s\omega_x \\ \omega_x\omega_z + s\omega_y & \omega_y\omega_z - s\omega_x & s^2 + \omega_z^2 \end{bmatrix}. \tag{A4b}$$

Furthermore, by closely inspecting above equations, it is clear that Ψ_1 and Ψ_2 are decomposed as

$$\Psi_1 = \frac{1}{s\left(s^2 + \|\boldsymbol{\omega}\|^2\right)} \left[(s^2 + \|\boldsymbol{\omega}\|^2) I_{3\times3} - s[\boldsymbol{\omega}\times] + [\boldsymbol{\omega}\times]^2 \right], \tag{A5a}$$

and

$$\Psi_2 = \frac{-1}{s^2\left(s^2 + \|\boldsymbol{\omega}\|^2\right)} \left[(s^2 + \|\boldsymbol{\omega}\|^2) I_{3\times3} - s[\boldsymbol{\omega}\times] + [\boldsymbol{\omega}\times]^2 \right]. \tag{A5b}$$

Next, The inverse Laplace transformation of Eq.(A3) is given by

$$\Phi = \begin{bmatrix} \Phi_1 & \Phi_2 \\ 0_{3\times3} & I_{3\times3} \end{bmatrix}, \tag{A6}$$

where

$$\Phi_1 = I_{3\times3} - [\boldsymbol{\omega}\times] \frac{\sin\left(\|\boldsymbol{\omega}\|\Delta t\right)}{\|\boldsymbol{\omega}\|} + [\boldsymbol{\omega}\times]^2 \frac{\left\{1 - \cos\left(\|\boldsymbol{\omega}\|\Delta t\right)\right\}}{\|\boldsymbol{\omega}\|^2}, \tag{A7a}$$

and

$$\Phi_2 = -\Delta t I_{3\times3} + [\boldsymbol{\omega}\times] \frac{\left\{1 - \cos\left(\|\boldsymbol{\omega}\|\Delta t\right)\right\}}{\|\boldsymbol{\omega}\|^2} - [\boldsymbol{\omega}\times]^2 \frac{\left\{\|\boldsymbol{\omega}\|\Delta t - \sin\left(\|\boldsymbol{\omega}\|\Delta t\right)\right\}}{\|\boldsymbol{\omega}\|^3}. \tag{A7b}$$

Let us define the angular vector and the magnitude of the vector as $\boldsymbol{\theta} = \boldsymbol{\omega}\Delta t$ and $\theta = \|\boldsymbol{\theta}\|$, respectively. Then, the sub-matrices of the state transition matrix can be rewritten as

$$\Phi_1 = I_{3\times3} - [\boldsymbol{\theta}\times] \frac{\sin\theta}{\theta} + [\boldsymbol{\theta}\times]^2 \frac{1 - \cos\theta}{\theta^2}, \tag{A8a}$$

and

$$\Phi_2 = -\Delta t \left(I_{3\times3} - [\boldsymbol{\theta}\times] \frac{1 - \cos\theta}{\theta^2} + [\boldsymbol{\theta}\times]^2 \frac{\theta - \sin\theta}{\theta^3} \right). \tag{A8b}$$

References

[1] Cho, A., Kim, J., Lee, S., Choi, S., Lee, B., Kim, B. and Kee, C., "Fully Automatic Taxiing, Takeoff and Landing of a UAV Using a Single-Antenna GPS Receiver Only", *Control, Automation and Systems*, ICCAS'07. International Conference on. IEEE, 2007.

[2] Babu, R. and Wang, J., "Improving the Quality of IMU-Derived Doppler Estimates for Ultra-Tight GPS/INS Integration", *GNSS2004*, 2004, pp. 16-19.

[3] Sabatini, A. M., "Quaternion-Based Extended Kalman Filter for Determining Orientation by Inertial and Magnetic Sensing", *IEEE Transactions on Biomedical Engineering*, Vol. 53, No. 7, 2006, pp. 1346-1356.

[4] Rong, Z., et al. "A Linear Fusion Algorithm for Attitude Determination Using Low Cost MEMS-based Sensors." *Measurement*, Vol. 40 No. 3, 2007, pp. 322-328.

[5] Lai, Y.-C., Jan, S.-S., and Hsiao, F.-B., "Development of A Low-cost Attitude and Heading Reference System Using A Three-axis Rotating Platform." *Sensors*, Vol. 10, No. 4, 2010, pp. 2472-2491.

[6] Roetenberg, D., et al. "Compensation of Magnetic Disturbances Improves Inertial and Magnetic Sensing of Human Body Segment Orientation." *Neural Systems and Rehabilitation Engineering, IEEE Transactions on*, Vol. 13, No. 3, 2005. pp. 395-405.

[7] Foxlin, E., "Inertial Head-tracker Sensor Fusion by A Complementary Separate-bias Kalman Filter." *Virtual Reality Annual International Symposium, Proceedings of the IEEE 1996*, 1996.

[8] Sabatini, A. M., "Quaternion-based Extended Kalman Filter for Determining Orientation by Inertial and Magnetic Sensing." *Biomedical Engineering, IEEE Transactions on*, Vol. 53 No. 7, 2006, pp. 1346-1356.

[9] Gebre-Egziabher, D., Hayward, R. C., and Powell, J. D., "Design of Multi-sensor Attitude Determination Systems." *Aerospace and Electronic Systems, IEEE Transactions on*, Vol. 40 No. 2, 2004, pp. 627-649..

[10] Li, W., and Wang, J., "Effective Adaptive Kalman Filter for MEMS-IMU/Magnetometers Integrated Attitude and Heading Reference Systems." *Journal of Navigation*, Vol. 66, No.01, 2013, pp. 99-113.

[11] Calusdian, J., Yun, X., and Bachmann, E., "Adaptive-gain Complementary Filter of Inertial and Magnetic Data for Orientation Estimation." *Robotics and Automation (ICRA), 2011 IEEE International Conference on*. IEEE, 2011.

[12] Crassidis, J. L., and Junkins, J. L., *Optimal Estimation of Dynamic Systems*, CRC press, 2011.

[13] Trawny, N., and Roumeliotis, S. I., "Indirect Kalman Filter for 3D Attitude Estimation." *University of Minnesota,*

Dept. of Comp. Sci. & Eng., Tech. Rep 2, 2005.

[14] Yun, X., et al. "An Improved Quaternion-based Kalman Filter for Real-time Tracking of Rigid Body Orientation." *Intelligent Robots and Systems, 2003.(IROS 2003). Proceedings. 2003 IEEE/RSJ International Conference on*. Vol. 2. IEEE, 2003.

[15] Diebel, J., "Representing Attitude: Euler angles, Unit Quaternions, and Rotation Vectors." *Matrix*, Vol.58 No.15-16, 2006, pp. 1-35.

[16] Pethel, S. J., "Test and Evaluation of High Performance Micro Electro-mechanical System Based Inertial Measurement Units." *Position, Location, And Navigation Symposium, 2006 IEEE/ION*. IEEE, 2006.

[17] Groves, P. D., *Principles of GNSS, Inertial, and Multisensor Integrated Navigation Systems*. Artech house, 2013.

DOI: http://dx.doi.org/10.5139/IJASS.2017.18.3.555